

The Impact of Histogram Equalization and Color Mapping on ResNet-34's Overall Performance for COVID-19 Detection

Jonathan David Freire
Yachay Tech University, Hacienda San
Jose, Urcuqui 100119, Ecuador

Jordan Rodrigo Montenegro
Yachay Tech University, Hacienda San
Jose, Urcuqui 100119, Ecuador

Hector Andres Mejia
Yachay Tech University, Hacienda San
Jose, Urcuqui 100119, Ecuador

Franz Paul Guzman
Yachay Tech University, Hacienda San
Jose, Urcuqui 100119, Ecuador

Carlos Enrique Bustamante
Arizona State University, Tempe, AZ
85281, United States

Ronny Xavier Velastegui
Norwegian University of Science and
Technology, Høgskoleringen 1,
Trondheim 7491, Norway and SDAS
Research Group
(www.sdas-group.com)

Lorena De Los Angeles Guachi
Department of Mechatronics
Universidad Internacional del
Ecuador, Av. Simon Bolivar 170411,
Ecuador and SDAS Research Group
(www.sdas-group.com)

ABSTRACT

The COVID-19 pandemic has had a “devastating” impact on public health and well-being around the world. Early diagnosis is a crucial step to begin treatment and prevent more infections. In this sense, early screening approaches have demonstrated that in chest radiology images, patients present abnormalities that distinguish COVID-19 cases. Recent studies based on Convolutional Neural Networks (CNNs), using radiology imaging techniques, have been proposed to assist in the accurate detection of COVID-19. Radiology images are characterized by the opacity produced by “ground glass” which might hide powerful information for feature analysis. Therefore, this work presents a methodology to assess the overall performance of Resnet-34, a deep CNN architecture, for COVID-19 detection when pre-processing histogram equalization and color mapping are applied to chest X-ray images. Besides, to enrich the available images related to COVID-19 studies, data augmentation techniques were also carried out. Experimental results reach the highest precision and sensitivity when applying global histogram equalization and pink color mapping. This study provides a point-of-view based on accuracy metrics to choose pre-processing techniques that can improve CNNs performance for radiology image classification purposes.

CCS CONCEPTS

• Computing methodologies; • Image processing;

KEYWORDS

COVID-19, Image pre-processing, ResNet-34

ACM Reference Format:

Jonathan David Freire, Jordan Rodrigo Montenegro, Hector Andres Mejia, Franz Paul Guzman, Carlos Enrique Bustamante, Ronny Xavier Velastegui, and Lorena De Los Angeles Guachi. 2021. The Impact of Histogram Equalization and Color Mapping on ResNet-34's Overall Performance for COVID-19 Detection. In *2021 4th International Conference on Data Storage and Data Engineering (DSDE '21)*, February 18–20, 2021, Barcelona, Spain. ACM, New York, NY, USA, 7 pages. <https://doi.org/10.1145/3456146.3456154>

1 INTRODUCTION

The rapid spread of the COVID-19 disease, which is caused by the SARS-CoV-2 virus, has caused panic worldwide since December 2019 [16]. At the moment, it is very difficult to stop the spread of the disease, mainly due to its transmission from person to person and its variable incubation period (which can last 14 days) [33].

Currently, a viral nucleic acid detection using real-time polymerase chain reaction (RT PCR) is the accepted standard diagnostic method for COVID-19. Its accuracy in COVID-19 detection is 94.44%, and its sensitivity reaches 88.24% [17]. However, many underdeveloped countries are unable to test for COVID-19 using PCR tests, mainly due to the cost of these tests. To mitigate the problem, several alternatives have been proposed. One of them is the use of chest X-ray images to detect, by using Convolutional Neural Networks (CNNs) based techniques, whether a person has COVID-19 or not. These techniques have demonstrated promising results in terms of accuracy, sensitivity and specificity [3, 25]. However, the most challenging problems in image processing, such as low contrast, regions with varied brightness, and features hidden in grayscale

Permission to make digital or hard copies of all or part of this work for personal or classroom use is granted without fee provided that copies are not made or distributed for profit or commercial advantage and that copies bear this notice and the full citation on the first page. Copyrights for components of this work owned by others than ACM must be honored. Abstracting with credit is permitted. To copy otherwise, or republish, to post on servers or to redistribute to lists, requires prior specific permission and/or a fee. Request permissions from permissions@acm.org.

DSDE '21, February 18–20, 2021, Barcelona, Spain

© 2021 Association for Computing Machinery.

ACM ISBN 978-1-4503-8930-3/21/02...\$15.00

<https://doi.org/10.1145/3456146.3456154>

images, are still an open issue for COVID-19 detection. Although some studies have concentrated on image enhancement techniques to tackle the low contrast problem [1, 10, 30], pre-processing tasks have not been widely explored.

This work introduces a methodology to evaluate the impact of pre-processing benchmark techniques, such as histogram equalization combined with color mapping, on the overall performance achieved by ResNet-34 CNN for COVID-19 detection. The global and local equalization of histograms aims to enhance image contrast, and false colors intend to produce a higher visual quality of chest image features that discriminate COVID-19 cases. ResNet-34 CNN is exploited as the classification model since it exhibits considerably lower training error and is generalizable to the validation data compared to other Residual Neural Networks [13]. This CNN model eases the optimization by providing faster convergence at an early stage. In addition, ResNet models have been successfully used in medical image analysis achieving great results in terms of accuracy [3, 11, 25, 31].

Besides, to enrich the available images related to COVID-19 studies (COVID-19 [8] and chest X-ray [24]), data augmentation techniques were also carried out. The obtained results demonstrated that an adequate pre-processing of the dataset, the precision and specificity of the explored neural network increase, reaching a reliable classification of chest X-ray images that belong to COVID-19 patients.

The rest of the paper is organized as follows. Section 2 describes most relevant related works. The dataset and the methodology used in this work are described in Section 3. Experimental setup is presented in Section 4. Results are presented and discussed in Section 5. Finally, Section 6 deals with the concluding remarks.

2 RELATED WORKS

Due to the COVID-19 pandemic, recent research has begun to explore CNN-based approaches for detecting COVID-19 cases from different modalities of medical imaging. Some works have treated COVID-19 detection as a binary classification task [2, 23, 26]. Authors in [25] evaluated InceptionV3, ResNet-50, and Inception-ResNetV2 to distinguish between Normal and COVID-19 cases. By contrast, other works treated COVID-19 detection as a multi-classification task [4, 7, 18, 27, 30]. For instance, COVID-19, common bacterial pneumonia and normal cases are distinguished in [3] by using several CNN architectures such as VGG19, MobileNet v2, Inception, Xception and Inception ResNet v2. Meanwhile, cases such as normal, viral pneumonia, bacterial pneumonia and COVID-19 have been also predicted by use of ResNet-50 network [11].

The lack of images regarding to COVID-19 cases has been faced by combining some public sources of X-ray images, radiology and CT snapshots [3, 8, 19, 21]. In this sense, [32] introduced an extensive dataset of 13975 images, which is a compilation from other open-source datasets and contains 358 X-ray images of COVID-19 cases. On the other hand, data augmentation techniques have been also exploited. For instance, in [20] and [22] generative adversarial networks (GAN) were applied to generate more images from the original dataset. This technique allowed the final dataset to be even 30 times larger than the originally collected dataset.

COVID-19 diagnosis demands high effectiveness; therefore, authors in [11] presented a 3-step technique to fine-tune a pre-trained ResNet-50 architecture to improve the model performance and reduce the training time. In the same context, [26] proposed random oversampling and a weighted class loss function approach for unbiased fine-tuned learning in various state-of-the-art deep learning approaches.

Other works have concentrated their efforts to introduce new CNN frameworks appropriated for COVID-19 detection. In this sense, [32] introduced COVID-Net, which is a deep convolutional neural network design tailored for the detection of COVID-19 cases from chest X-ray (CXR). In [14], the authors present COVIDX-Net framework to automatically identify COVID-19 cases based on seven deep learning classifiers: namely VGG19, DenseNet121, ResNetV2, InceptionV3, Inception ResNetV2, Xception, and MobileNetV2. A methodology proposed in [29], introduced COVID-SDNet, which is a modification of Resnet-50 initialized with ImageNet weights. Four variations of AlexNet were studied in [27] to test how the modification of the layers outperforms pre-trained AlexNet models in small datasets.

Although some studies have focused on applying enhancement techniques to manage the low contrast of the images before using them to feed deep learning models, typical pre-processing tasks performed histogram-based techniques. For instance, [30] applied three image enhancement techniques to improve the contrast in the images: contrast limited adaptive histogram equalization (CLAHE), image complementation, and a mixture of the previous techniques together with raw images. The images resulting were used as input to SqueezeNet, ResNet18, Inception-v3, and DenseNet201 models. In addition, [1] performed pre-processing with histogram modification to handle the low contrast in the images and [10] performed intensity normalization and CLAHE algorithm. Hence, this work evaluates the performance achieved by combining histogram-based with map coloring techniques.

3 MATERIALS AND METHODS

3.1 Dataset

To evaluate the proposed methodology, this work used COVID-19 [8] and Chest X-ray [24] databases. COVID-19 database contains X-ray and CT chest images of patients diagnosed with COVID-19 and other viral and bacterial pneumonia such as severe acute respiratory syndrome (SARS), and acute respiratory distress syndrome (ARDS). From this database, 95 COVID-19 images and 19 images of bacterial pneumonia were extracted. In order to improve the overall performance of the proposed methodology, 81 images of healthy patients and 41 images of pneumonia were used from the Chest X-ray database. In all cases, images were resized to 224*224 pixels and normalized with mean and variance from ImageNet [9] since the original weights of ResNet-34 belong to that database. In this work, SARS, ARDS, bacterial pneumonia, and healthy images were labeled as “No COVID-19” cases, resulting in a raw balanced dataset with two classes: “COVID-19” and “No COVID-19”. This dataset contains 234 images, 154 for training, with the remaining for testing purposes. Samples of chest images in patients with pneumonia cases are depicted in Figure 1

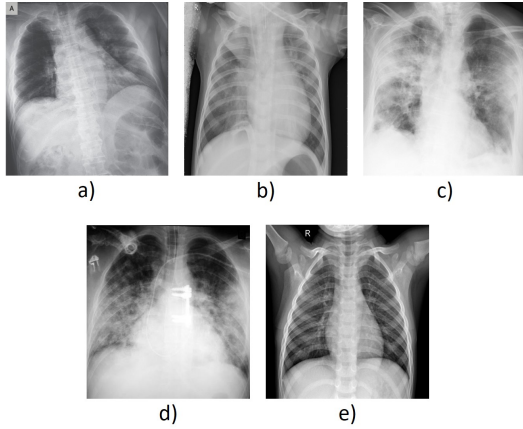


Figure 1: Samples related to: a) COVID-19; b) Bacterial pneumonia (No-COVID-19); c) SARS (No-COVID-19); d) ARDS (No-COVID-19); and e) Healthy cases (No-COVID-19)

3.2 Methodology

In the proposed methodology, after collecting images, a pre-processing phase for image enhancement was carried out. It consists of Histogram Equalization, and Color Mapping techniques. Then, a data augmentation task is performed to increase the quantity of data. Finally, pre-processed images are used as input to Resnet-34 for training and testing purposes. The general workflow of the proposed methodology is schematized in Figure 2

3.2.1 Preprocessing.

1. **Histogram Equalization:** This work explores the effectiveness of global and local techniques for COVID-19 diagnosis, considering that global histogram equalization (GHE) enhances image contrast; however, it often fails to adapt local image brightness features. On the other hand, contrast limited adaptive histogram equalization (CLAHE) is appropriated for handling local brightness features, but it usually suffers from blocking artifacts or halo and demands more computational power. Histogram equalization is given by Equation 1. It spreads the intensity frequencies in an equal range across the whole region [12] (or image in global histogram cases).

$$s_k = T(r_k) = (L - 1) \sum_{j=0}^k p_r(r_j) = \frac{(L - 1)}{MN} \sum_{j=0}^k n_j \quad (1)$$

2. **Color Mapping:** Color provides powerful information for feature analysis. In fact, the ability to distinguish pneumonia cases is essentially related with the way of representing colors in the processed images. In particular, features that discriminate viral pneumonia, such as COVID-19 cases are characterized by small white lines called peripheral ground glass [5]. Therefore, hot color mapping and pink color mapping are explored aiming at highlighting the features present in the images. Some of the results obtained from the dataset are depicted in Figure 3

3.2.2 Classification Model.

1. **Data Augmentation:** For training purposes, CNN demands huge amounts of varied data, otherwise the model may be not robust or might be prone to over-fitting. In this sense, and aiming at representing images taken with varied illumination and from different distances, the raw dataset is increased by performing pre-processing operations such as: random lighting (with a probability of 75%), random zoom (between 100% and 110% with a probability of 75%), random horizontal rotations (with a maximum of 25 degrees and a probability of 50%), and random warp (between -20 % and + 20% with a probability of 75%).
2. **Residual Neural Network:** To automatically classify chest images into COVID-19 and No-COVID-19 cases, this phase uses ResNet-34, a computer vision approach for image classification. Residual Neural Network (ResNet) is a deep CNN architecture, which eases the optimization by providing faster convergence at an early stage [13]. ResNet is characterized by residual blocks (3-by-3 convolution block followed by two-point convolution layers) whose function according to [13] is to avoid the degradation problem where apparently the shallower networks learn much better. The output of each block is added to the output of the previous block as depicted in Figure 4. A residual block mathematically is defined according to Equation 2.

$$y = F(x, W_i) + x \quad (2)$$

Where x and y are the input and output vectors of the layers and the function $F(x, W_i) + x$ represents the residual mapping that has to be learned.

In summary, the basis of a residual network consists in adding, every certain number of layers, the output of a previous layer to the output of a latter one. Which also will be added to the output of

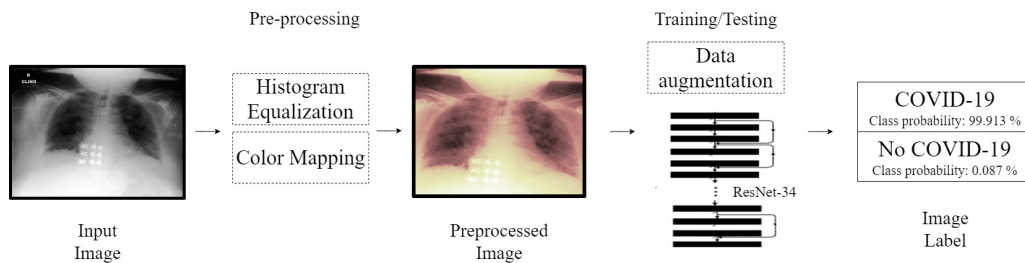


Figure 2: General workflow of the proposed methodology

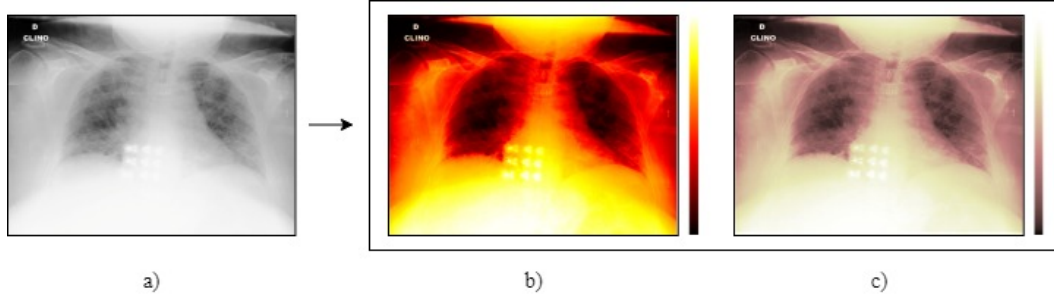


Figure 3: Image samples related to: a) Chest image; b) Chest image with hot color map; and c) Chest image with pink color map

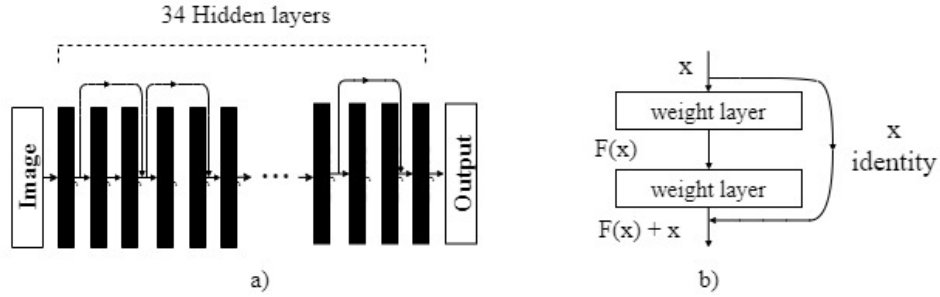


Figure 4: ResNet-34 Model. a) Model structure; b) Residual block representation

Table 1: Description of all the experiments

Experiment		Pre-processing Features				
		Data augmentation	Histogram Equalization		Color mapping	
			GHE	CLAHE	Hot	Pink
1	✓					
2	✓	✓				
3	✓		✓			
4	✓	✓		✓		
5	✓	✓			✓	
6	✓		✓	✓		
7	✓		✓		✓	

the next group of layers. An example of a 34-layer residual network can be seen in Figure 4

4 EXPERIMENTAL SETUP

Python software routines were implemented to test the proposed methodology. Experiments were done, using Fast.ai library [15] for fast and accurate training of neural networks and OpenCV library [6] for high performance when working with images on a Tesla K80 GPU provided by a free-of-charge version of Google Colab. Data augmentation task has been applied in all experimental tests aiming at avoiding over-fitting caused by small dataset [10]. To evaluate the influence of pre-processing algorithms on the overall performance achieved by ResNet-34, this work processed the chest X-ray images through 7 experiments as is shown in Table 1.

Each experiment was divided into 2 stages: pre-processing and classification. In the first stage, pre-processing of images was carried out applying histogram equalization and map coloring as shown in Table 1, later in the next stage ResNet-34 was used to perform the classification.

All experiments were performed using the following ResNet-34 hyperparameters: cyclic learning rate [28] from $1e^{-4}$ to $1e^{-3}$, applying $1e^{-4}$ to the layer 1 and $1e^{-3}$ to the layer 34; epochs=10; and batch size = 16. These hyperparameters were chosen experimentally.

The ability to correctly classify an input image as COVID-19 or No-COVID-19 is measured in terms of accuracy, precision, sensitivity and specificity given by Equations 3, 4, 5, and 6, respectively.

$$Accuracy = \frac{TP + TN}{(TP + FP + FN + TN)} \quad (3)$$

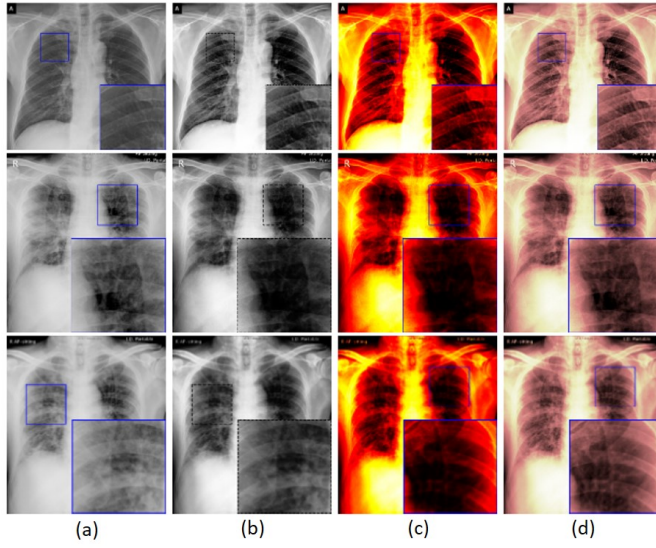


Figure 5: (a) Input images; (b) GHE applied on (a); (c) HOT Color mapping; (d) PINK Color mapping

$$\text{Precision} = \frac{TP}{TP + FP} \quad (4)$$

$$\text{Sensitivity} = \frac{TP}{TP + FN} \quad (5)$$

$$\text{Specificity} = \frac{TN}{TN + FP} \quad (6)$$

Where

TP represent COVID-19 cases correctly classified as COVID-19 ones.

FN represent No-COVID-19 cases wrongly classified as COVID-19 ones.

TN represent COVID-19 cases correctly classified as No-COVID-19 ones.

FP represent No-COVID-19 cases correctly classified as No-COVID-19 ones.

The developed code used for testing is available online at: <https://github.com/Jorel22/PreprocessingResnet34>

5 RESULTS AND DISCUSSION

Some of the outputs obtained from pre-processing algorithms are depicted in Figure 5 and Figure 6. It can be observed that the global equalization technique leads to a significant improvement in details Figure 5b, such as the bone structure and lungs, which edges are sharper. Also, these images appear more focused as opposed to the raw images in Figure 5a, which have more diffused edges. In addition, color mapping accentuates the difference between areas that have low contrast allowing the CNN to detect patterns easier. In particular, pink color mapping preserves more detail as opposed of hot color mapping where low contrast areas appear darker as can be seen in Figure 5c.

On the other hand, images resulting from contrast limited adaptive histogram equalization had a slight general improvement, it is useful since it enhances the details of the chest structures with a

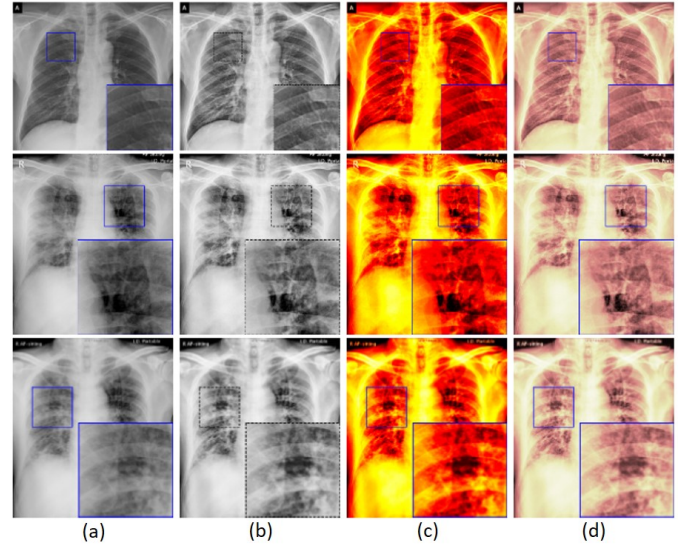


Figure 6: (a) Input images; (b) CLAHE applied on (a); (c) HOT Color mapping; (d) PINK Color mapping

minimal change in the image, as can be seen in Figure 6. However, clipping in the intensity values produced by CLAHE reduces the differences in the overall contrast so when color mapping is applied the images become noisier and the process ineffective in both cases: Figure 6c and Figure 6d.

Each experiment was performed four times, and the resulting averages are summarized in Figure 7. As can be seen, the highest sensitivity is achieved by experiments 1) only data augmentation, 4) GHE + Hot Map, 6) CLAHE + Hot Map, and 7) CLAHE + Pink Map. Since sensitivity and precision are focused on the proportion of positive COVID-cases, pre-processing combinations with the highest precision and sensitivity are expected. In this sense, 5) GHE + Pink Map experiment reaches the best trade-off between sensitivity and precision metrics. These results make sense since the improvement in the image's details achieved by GHE is greater than that of CLAHE; and the pink color mapping does not introduce as many dark zones as hot color mapping does.

In addition, experiment 5 reports the highest specificity value with the most samples correctly classified as non-relevant in a one-vs-all classification perspective. All the results confirm the benefit of combining color mapping with histogram equalization techniques.

6 CONCLUSION

The impact of pre-processing benchmark techniques on the overall performance of ResNet-34 CNN for COVID-19 detection has been addressed in this study. Techniques such as histogram equalization combined with color mapping have been applied. Specifically, there are improvements in metrics such as precision and sensitivity of ResNet-34, compared to using images without those pre-processing techniques, when determining whether a chest X-ray image belongs to a person who has COVID-19 or not.

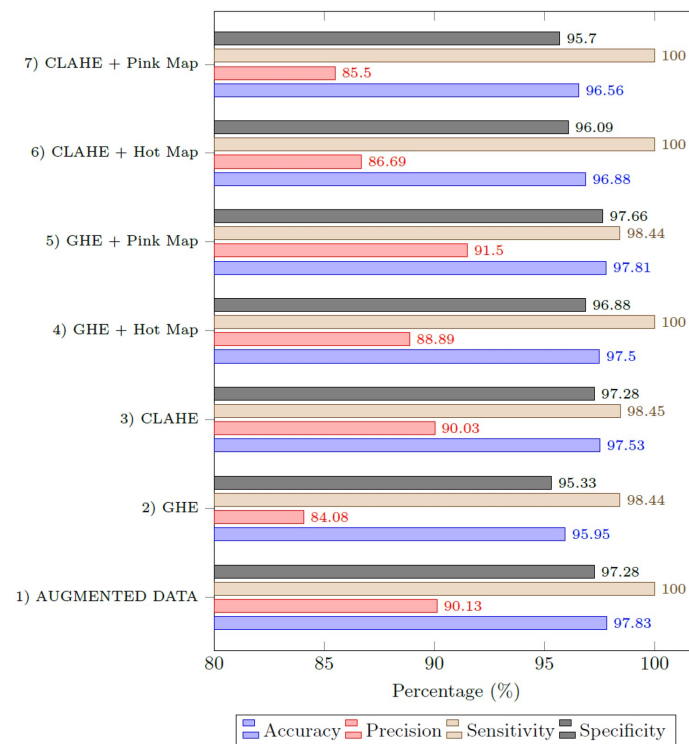


Figure 7: Overall results of pre-processing and ResNet 34 hyper parameters tuning

To test histogram equalization techniques, global histogram equalization and local histogram equalization were used, while color map pink and color map hot were used to test color mapping. Different combinations were made with these techniques, as can be seen in Table 1. It was finally possible to see that the use of global histogram equalization with color map pink achieved the best overall performance: 97.81% accuracy, 91.5% precision, 98.44% sensitivity and 97.66% specificity.

With the results presented in this work, it is expected that these pre-processing techniques become more popular in order to obtain more reliable results. Finally, future works include increasing the dataset used for training and apply cold color mappings for pre-processing. Also, we will explore the effects of those pre-processing techniques with other different CNN Architectures such as Alexnet, DenseNet, VGG, Inception, among others.

REFERENCES

- [1] Asmaa Abbas, Mohammed M Abdelsamea, and Mohamed Medhat Gaber. 2020. Classification of COVID-19 in chest X-ray images using DeTraC deep convolutional neural network. arXiv preprint arXiv:2003.13815(2020). Sam Anzaroot and Andrew McCallum. 2013. UMass Citation Field Extraction Dataset. Retrieved May 27, 2019 from <http://www.iesl.cs.umass.edu/data/data-umasscitationfield>
- [2] Mete Ahishali, Aysen Degerli, Mehmet Yamac, Serkan Kiranyaz, Muhammad EHChowdhury, Khalid Hameed, Tahir Hamid, Rashid Mazhar, and Moncef Gabouj. 2020. A Comparative Study on Early Detection of COVID-19 from Chest X-Ray Images. arXiv preprint arXiv:2006.05332(2020). Chelsea Finn. 2018. Learning to Learn with Gradients. PhD Thesis, EECS Department, University of Berkeley.
- [3] Ioannis D Apostolopoulos and Tzani A Mpesiana. 2020. Covid-19: automatic detection from x-ray images utilizing transfer learning with convolutional neural networks. *Physical and Engineering Sciences in Medicine* (2020), 1. <https://doi.org/10.1016/j.cell.2018.02.010>
- [4] Sohaib Asif, Yi Wenhui, Hou Jin, Yi Tao, and Si Jinhai. 2020. Classification of COVID-19 from Chest X-ray images using Deep Convolutional Neural Networks. medRxiv(2020).
- [5] Gary T Barnes and Karen Lauro. 1989. Image processing in digital radiography: basic concepts and applications. *Journal of digital imaging* 2, 3 (1989), 132. <https://doi.org/10.1007/BF03168032>
- [6] G. Bradski. 2000. The OpenCV Library. Dr. Dobb's Journal of Software Tools (2000).
- [7] Luca Brunese, Francesco Mercaldo, Alfonso Reginelli, and Antonella Santone. 2020. Explainable deep learning for pulmonary disease and coronavirus COVID-19 detection from X-rays. *Computer Methods and Programs in Biomedicine* (2020), 105608. <https://doi.org/10.1016/j.cmpb.2020.105608>
- [8] Joseph Paul Cohen, Paul Morrison, and Lan Dao. 2020. COVID-19 image data collection. arXiv 2003.11597(2020). <https://github.com/ieee8023/covid-chestxray-dataset>
- [9] Jia Deng, Wei Dong, Richard Socher, Li-Jia Li, Kai Li, and Li Fei-Fei. 2009. Imagenet: A large-scale hierarchical image database. In 2009 IEEE conference on computer vision and pattern recognition. Ieee, 248–255. <https://doi.org/10.1109/CVPR.2009.5206848>
- [10] Khalid Elasnou and Youness Chawki. 2020. Using X-ray images and deep learning for automated detection of coronavirus disease. *Journal of Biomolecular Structure and Dynamics* just-accepted (2020), 1–22. <https://doi.org/10.1007/s10489-020-01829-7>
- [11] Muhammad Farooq and Abdul Hafeez. 2020. Covid-resnet: A deep learning frame-work for screening of covid19 from radiographs. arXiv preprint arXiv:2003.14395(2020).
- [12] Rafael C Gonzales and Richard E Woods. 2008. Digital image processing.
- [13] Kaiming He, Xiangyu Zhang, Shaoqing Ren, and Jian Sun. 2016. Deep Residual Learning for Image Recognition. 770–778. <https://doi.org/10.1109/CVPR.2016.90>
- [14] Ezz El-Din Hemdan, Marwa A Shouman, and Mohamed Esmail Karar. 2020. Covidx-net: A framework of deep learning classifiers to diagnose covid-19 in x-ray images. arXiv preprint arXiv:2003.11055(2020)
- [15] Jeremy Howard et al. 2018. fastai. <https://github.com/fastai/fastai>
- [16] Chaolin Huang, Yeming Wang, Xingwang Li, Lili Ren, Jianping Zhao, Yi Hu, LiZhang, Guohui Fan, Jiuyang Xu, Xiaoying Gu, Zhenshun Cheng, Ting Yu, JiaanXia, Yuan Wei, Wenjuan Wu, Xuelei Xie, Wen Yin, Hui Li, Min Liu, and Bin Cao. 2020. Clinical features of patients infected with 2019 novel coronavirus in Wuhan, China. *The Lancet* 395 (01 2020). [https://doi.org/10.1016/S0140-6736\(20](https://doi.org/10.1016/S0140-6736(20)

- 30183-5
- [17] Farzaneh Jalalypour, Safar Farajnia, Mohammad Hossein Somi, Zoya Hojabri, Rana Yousefzadeh, and Nazli Saeedi. 2016. Comparative Evaluation of RUT, PCR and ELISA Tests for Detection of Infection with Cytotoxigenic *H. pylori*. *Advanced pharmaceutical bulletin* 6, 2 (2016), 261. <https://doi.org/10.15171/apb.2016.036>.
 - [18] Cheng Jin, Weixiang Chen, Yukun Cao, Zhanwei Xu, Xin Zhang, Lei Deng, Chuansheng Zheng, Jie Zhou, Heshui Shi, and Jianjiang Feng. 2020. Development and Evaluation of an AI System for COVID-19 Diagnosis. *medRxiv*(2020). <https://doi.org/10.1101/2020.03.20.20039834>.
 - [19] Daniel Kermany, Kang Zhang, Michael Goldbaum. 2018. Labeled Optical Coherence Tomography (OCT) and Chest X-Ray Images for Classification. *Mendeley Data*, V2, <https://doi.org/10.17632/rscbjbr9sj.2>.
 - [20] Nour Eldeen M Khalifa, Mohamed Hamed N Taha, Aboul Ella Hassanien, and Sally Elghamrawy. 2020. Detection of coronavirus (COVID-19) associated pneumonia based on generative adversarial networks and a fine-tuned deep transfer learning model using chest X-ray dataset. *arXiv preprint arXiv:2004.01184*(2020)
 - [21] Larxel. 2020. COVID-19 X rays. <https://www.kaggle.com/andrewmvd/conv19-X-rays>
 - [22] Mohamed Loey, Florentin Smarandache, and Nour Eldeen M Khalifa. 2020. Within the Lack of Chest COVID-19 X-ray Dataset: A Novel Detection Model Based on GAN and Deep Transfer Learning. *Symmetry* 12, 4 (2020), 651. <https://doi.org/10.3390/sym12040651>
 - [23] Pranali Manapure, Kiran Likhari, and Hemlata Kosare. [n.d.]. Detecting COVID-19 in X-ray images with Keras, Tensor Flow, and Deep Learning. *assessment2*[n.d.], 3.
 - [24] Paul Mooney. 2018. Chest X-Ray Images (Pneumonia). <https://www.kaggle.com/paultimothymooney/chest-xray-pneumonia>.
 - [25] Ali Narin, Ceren Kaya, and Ziyne Pamuk. 2020. Automatic detection of coronavirus disease (covid-19) using x-ray images and deep convolutional neural networks. *arXiv preprint arXiv: 2003.10849*(2020).
 - [26] Narinder Singh Punj and Sonali Agarwal. 2020. Automated diagnosis of COVID-19 with limited posteroanterior chest X-ray images using fine-tuned deep neural networks. *arXiv preprint arXiv:2004.11676*(2020).
 - [27] Shadman Q Salih, Hawre Kh Abdulla, Zaneer Sh Ahmed, Nigar M Shafiq Surameery, and Rasper Dh Rashid. 2020. Modified AlexNet Convolution Neural Network for Covid-19 Detection Using Chest X-ray Images. *Kurdistan Journal of Applied Research* (2020), 119–130. <https://doi.org/10.1101/2020.05.01.20088211>
 - [28] Leslie N. Smith and Nicholay Topin. 2019. Super-convergence: very fast training of neural networks using large learning rates. In *Artificial Intelligence and Machine Learning for Multi-Domain Operations Applications*, Tien Pham (Ed.), Vol. 11006. International Society for Optics and Photonics, SPIE, 369 – 386. <https://doi.org/10.1117/12.2520589>
 - [29] Siham Tabik, Anabel Gomez-Rios, JL Martin-Rodriguez, I Sevillano-Garcia, Manuel Rey-Area, D Charte, Emilio Guirado, JL Suarez, Julian Luengo, MA Valero-Gonzalez, *et al.* 2020. COVIDGR dataset and COVID-SDNet methodology for predicting COVID-19 based on Chest X-Ray images. *arXiv preprint arXiv: 2006.01409*(2020).
 - [30] Anas Tahir, Yazan Qiblawey, Amith Khandakar, Tawsifur Rahman, Uzair Khurshid, Faray Musheravati, Serkan Kiranyaz, and Muhammad EH Chowdhury. 2020. Coronavirus: Comparing COVID-19, SARS and MERS in the eyes of AI. *arXiv preprint arXiv:2005.11524*(2020).
 - [31] Muhammed Talo, Özal yıldırım, Ulas Baloglu, Galip Aydin, and U Rajendra Acharya. 2019. Convolutional neural networks for multi-class brain disease detection using MRI images. *Computerized Medical Imaging and Graphics* 78 (102019), 101673. <https://doi.org/10.1016/j.compmedimag.2019.101673>.
 - [32] Linda Wang and Alexander Wong. 2020. COVID-Net: A tailored deep convolutional neural network design for detection of COVID-19 cases from chest radiography images. *arXiv*(2020), arXiv–2003.
 - [33] WHO. 2020. QA on coronaviruses (COVID-19). <https://www.who.int/emergencies/diseases/novel-coronavirus-2019/question-and-answers-hub/q-a-detail/q-a-coronaviruses>.